

## Loss of the Chromosomal Region 10q23–25 in Prostate Cancer<sup>1</sup>

Ian C. Gray,<sup>2</sup> Stewart M. A. Phillips, Susan J. Lee, John P. Neoptolemos, Jean Weissenbach, and Nigel K. Spurr

Imperial Cancer Research Fund, Clare Hall Laboratories, South Mimms, Potters Bar, Herts EN6 3LD, United Kingdom [I. C. G., N. K. S.]; Department of Surgery, Queen Elizabeth Hospital, Edgbaston, Birmingham B15 2TH, United Kingdom [S. M. A. P., J. P. N.]; Central Manchester Healthcare National Health Service Trust, St. Mary's Hospital for Women and Children, Manchester M13 0JH, United Kingdom [S. J. L.]; and Genethon, 1 rue de l'Internationale, 91000 Evry, France [J. W.]

### Abstract

Loss of the chromosomal region 10q23–25 is a frequent event in the progression of prostate adenocarcinoma. A candidate tumor suppressor gene from this region, *Mxi1* at 10q25, has recently been shown to be mutated in a small number of prostate tumors. To more strictly define those regions of 10q loss that are likely to be involved in tumor advancement, we have constructed a detailed deletion map spanning 10q23–25 that incorporates *Mxi1*. Sixty-two % (23 of 37) of tumors analyzed exhibited some degree of 10q23–25 loss. Our data suggest the presence of a prostate tumor suppressor gene(s) near the 10q23–24 boundary, which was deleted in the overwhelming majority (22 of 23) of tumors showing loss. In contrast, specific loss of *Mxi1*, as opposed to loss of other 10q23–25 regions or of the entire region, was observed in only 1 of 23 tumors and was accompanied by loss of markers at the 10q23–24 boundary. Furthermore, we failed to detect any mutations in *Mxi1* in those tumors showing *Mxi1*-associated marker loss by either single-strand conformation polymorphism analysis or direct DNA sequencing.

### Introduction

Cytogenetic and allelic loss studies have pointed to a number of chromosomal regions of potential involvement in prostate cancer, most notably 8p, 16q, and 10q (see Ref. 1 for a recent review). More specifically, a number of tumors exhibit precise loss of the region 10q23–25 (2, 3), strongly suggesting the presence of a tumor suppressor gene in this area. One candidate gene residing at 10q25 is *Mxi1*, which encodes a negative regulator of the Myc oncoprotein (4); potentially disabling mutations of *Mxi1* in a limited number of prostate tumors have recently been described. However, mutations were detected in only a small percentage of cells from each tumor (5), and the impact of loss of function of *Mxi1* in a small subpopulation of cells within the tumor is unclear.

Using fluorescence-based allelotyping with highly informative microsatellite CA repeat markers, we have generated a detailed deletion map spanning 10q23–25, allowing stricter definition of the region of 10q loss likely to be involved in tumor advancement. In addition, we have assessed the frequency of loss and mutation of *Mxi1* in prostate tumors to clarify the role of this gene in prostate tumor progression.

### Materials and Methods

**DNA Preparation.** Tumors and venous blood samples were obtained from men undergoing transurethral resection of the prostate. Tumor tissue was microdissected away from normal tissue, and tumor and blood DNA were prepared as described previously (6).

**PCR.** PCR was performed in 50- $\mu$ l reactions containing 30 ng template DNA, 1 $\times$  PCR buffer (Boehringer Mannheim), 20 pmol primer, 200  $\mu$ M dNTPs (Boehringer Mannheim), and 1 unit of Taq polymerase (Boehringer Mannheim) on a GeneAmp 9600 thermal cycler (Perkin Elmer Cetus). For

amplification of microsatellite CA repeat markers (7), one of the primers was tagged with a fluorescent label (JOE, FAM, HEX, or TAMRA; Applied Biosystems). Microsatellite reaction mixtures were given 30 cycles of 30 s at 94°C, 30 s at 55°C, and 30 s at 72°C, preceded by a 3-min hot start at 95°C. The annealing temperature was lowered to 50°C for amplification of *Mxi1* helix-loop-helix and leucine zipper exons (5) and increased to 60° for amplification of the 3' exon; primer sequences for 3' exon amplification are 5'-GAGATTGAAGTGGATGTTGAAAG-3' (A) and 5'-AAATACAGGTC-CTCTGACCC-3' (B) and give a 319- or 324-bp product. To facilitate fluorescence-based typing of the (CAAAA)<sub>n</sub> polymorphism, primer A was tagged with FAM.

**Allele Typing.** Microsatellite allele sizes and loss of heterozygosity were determined by size separation of PCR products in a 6% denaturing polyacrylamide gel in the presence of a 2500-ROX size standard (Applied Biosystems) and detection with an 373A DNA sequencer running Genescan software (Applied Biosystems), following the manufacturer's guidelines. Up to 10 markers, distinguishable by size or fluorescent tag, were typed simultaneously. The resulting data were analyzed using Genotyper software (Applied Biosystems).

**SSCP.**<sup>3</sup> After amplification of *Mxi1* introns, 10  $\mu$ l of PCR products were mixed with 10  $\mu$ l formamide and heated to 90°C for 3 min. The denatured products were run in a 6% nondenaturing polyacrylamide gel at 25 W for 4–6 h with fan-assisted cooling to maintain a temperature of less than 25°C (8). DNA was transferred to a nylon membrane (Hybond N+; Amersham) and hybridized at 68°C for 3–4 h with a mixture of both PCR primers after end labeling with [<sup>32</sup>P]dCTP (Amersham) using terminal transferase (GIBCO-BRL). After washing in 2 $\times$  SSC/0.1% SDS for 5–10 min, filters were exposed to X-ray film for 1–24 h at –70°C.

**DNA Sequencing.** After purification by passage through a Centricon-100 column (Amicon), PCR-amplified *Mxi1* exons were sequenced using a PRISM cycle sequencing kit (Applied Biosystems) and a 373A DNA sequencer running 373A collection and analysis software (Applied Biosystems) in accordance with the manufacturer's instructions. Each exon was sequenced twice (once from each end) from independent PCR reactions. Sequence electropherograms were aligned using Sequence Navigator software (Applied Biosystems) and were compared by eye.

### Results

A total of 37 prostate tumors of various and histopathological grades and stages (Table 1) was typed for loss of heterozygosity at 24 CA repeat markers spanning 10q23–25 (7). Tumor tissue was microdissected away from normal tissue before DNA extraction, and tumor microsatellite profiles were compared to those from lymphocyte DNA to determine allelic loss. Eight samples of benign hyperplastic tissue were also studied. We considered a tumor DNA sample to be showing allelic loss if a reproducible signal reduction of greater than 20% as compared to normal tissue was observed, although in practice the degree of reduction was frequently much greater and in some instances approached 100%. Examples of allelic loss are shown in Fig. 1. A total of 23 tumors (62%) showed allelic loss at one or more markers on 10q23–25 (Table 1). Of these, 8 showed loss at all informative markers typed, and of these 8, a further 5 also showed

Received 7/31/95; accepted 9/20/95.

The costs of publication of this article were defrayed in part by the payment of page charges. This article must therefore be hereby marked *advertisement* in accordance with 18 U.S.C. Section 1734 solely to indicate this fact.

<sup>1</sup> Supported by the Imperial Cancer Research Fund.

<sup>2</sup> To whom requests for reprints should be addressed.

<sup>3</sup> The abbreviations used are: SSCP, single-strand conformation polymorphism; YAC, yeast artificial chromosome.

Table 1 Prostate tumors assessed for 10q23–25 loss

Tumor	Stage <sup>a</sup>	Grade <sup>b</sup>	Patient age	10q loss <sup>c</sup>
1	T <sub>1</sub> M <sub>0</sub>	2	81	+ (0.56)
2	T <sub>2</sub> M <sub>0</sub>	2	84	+ (0.53)
3	T <sub>2</sub> M <sub>0</sub>	1	67	+ (0.51)
4	T <sub>2</sub> M <sub>0</sub>	3	70	-
5	T <sub>2</sub> M <sub>0</sub>	3	59	-
6	T <sub>2</sub> M <sub>0</sub>	2	64	+ (0.49)
7	T <sub>2</sub> M <sub>1</sub>	3	84	-
8	T <sub>2</sub> M <sub>1</sub>	3	83	+ (0.79)
9	T <sub>2</sub> M <sub>1</sub>	3	71	-
10	T <sub>2</sub> M <sub>1</sub>	2	83	-
11	T <sub>2</sub> M <sub>1</sub>	2	78	+ (0.35)
12	T <sub>3</sub> M <sub>0</sub>	3	65	IS
13	T <sub>3</sub> M <sub>0</sub>	3	67	+ (0.65)
14	T <sub>3</sub> M <sub>0</sub>	2	79	+ (0.46)
15	T <sub>3</sub> M <sub>0</sub>	2	83	+ (0.52)
16	T <sub>3</sub> M <sub>0</sub>	2	72	+ (0.36)
17	T <sub>3</sub> M <sub>1</sub>	2	76	+ (0.37)
18	T <sub>3</sub> M <sub>1</sub>	3	73	+ (0.60)
19	T <sub>3</sub> M <sub>1</sub>	2	73	-
20	T <sub>3</sub> M <sub>1</sub>	3	61	-
21	T <sub>3</sub> M <sub>1</sub>	1	80	+ (0.57)
22	T <sub>3</sub> M <sub>1</sub>	2	64	+ (0.34)
23	T <sub>3</sub> M <sub>1</sub>	3	71	+ (0.25)
24	T <sub>3</sub> M <sub>1</sub>	1	65	+ (0.56)
25	T <sub>3</sub> M <sub>1</sub>	2	68	+ (0.38)
26	T <sub>4</sub> M <sub>0</sub>	3	72	-
27	T <sub>4</sub> M <sub>0</sub>	3	73	+ (0.54)
28	T <sub>4</sub> M <sub>0</sub>	3	55	-
29	T <sub>4</sub> M <sub>0</sub>	3	78	-
30	T <sub>4</sub> M <sub>1</sub>	3	64	+ (0.34)
31	T <sub>4</sub> M <sub>1</sub>	3	58	+ (0.58)
32	T <sub>4</sub> M <sub>1</sub>	3	71	+ (0.36)
33	T <sub>4</sub> M <sub>1</sub>	3	67	-
34	T <sub>4</sub> M <sub>1</sub>	3	67	-
35	T <sub>4</sub> M <sub>1</sub>	1	80	-
36	T <sub>4</sub> M <sub>1</sub>	2	75	+ (0.62)
37	T <sub>4</sub> M <sub>1</sub>	3	66	+ (0.38)

<sup>a</sup> Staging is based on digital rectal examination and bone scan (9).

<sup>b</sup> WHO gradings: 1, well differentiated; 2, moderately differentiated; 3, poorly differentiated; 4, mixture of differentiation.

<sup>c</sup> + = 10q loss; - = no detected 10q loss. IS, instability. Figures in parentheses give the average degree of signal reduction for microsatellite markers showing allele loss, as determined by fluorescence-based typing.

allelic loss at markers on the p arm, suggesting absence of the entire chromosome, possibly through nondisjunction. The allelic loss data are summarized in Fig. 2. No loss was seen in the benign hyperplastic tissue samples. One tumor showed microsatellite instability at the majority of loci (21 of 24; see Fig. 1), presumably due a defective DNA mismatch correction system (10). There is no clear correlation of loss of 10q with tumor stage or grade, suggesting that 10q losses may occur at any time during tumor progression.

The retinol-binding protein 4 gene (*RBP4*) and the cytochrome P450IIC gene cluster (*CYP2C*) were positioned on the deletion map after the identification of YAC clones bearing both these loci and adjacent microsatellite markers *D10S185* and *D10S571* (11). The map clearly reveals a common region of deletion proximal to *RBP4* and *CYP2C*, both of which have been cytogenetically mapped to 10q23–24 and 10q24.1, respectively (Refs. 12 and 13; Fig. 2). This region is lost in all of the tumors showing 10q loss in our study, with the exception of tumor 37, which was not informative for the markers from this area. Tumors 1, 3, 6, 13, 14, and 15 define a minimal region of deletion between markers AFMa124wd9 and *D10S583*, a distance of approximately 9 cM.

Eagle *et al.* (5) have recently identified mutations in the *Mxi1* gene at 10q25 in a small number of prostate tumors, leading to speculation that *Mxi1* can act as a tumor suppressor. We were able to place *Mxi1* on the deletion map after confirming its presence on Centre d'Etude du Polymorphisme Humain mega-YACs 936-h-5 and 966-h-9, which have been shown to overlap with YACs bearing the microsatellite marker *D10S597* (14). Only two tumors, 1 and 11, showed specific

loss of markers immediately flanking *Mxi1*; in both cases, this was in conjunction with allelic loss in the AFMa124wd9-*D10S583* region (Fig. 2).

In an attempt to further clarify the role of *Mxi1* loss in tumor progression, we screened tumors 1 and 11, and those tumors showing loss of the entire region, for *Mxi1* mutations by PCR amplification of individual exons, followed by SSCP analysis (8). Primers for PCR amplification of exons encoding helix-loop-helix and leucine zipper domains were taken from Eagle *et al.* (5). For amplification of the final 3' exon, primers derived from the immediate 5' end of the exon and from within the 3'-untranslated sequence were used (4, 5). These 3 pairs of primers give 66% coverage of the coding sequence of *Mxi1*. The genomic structure of the 5' end of the *Mxi1* gene has not yet been determined; we were, therefore, unable to analyze exons 5' to the helix-loop-helix domain. SSCP analysis failed to detect any mutations in the two-thirds of *Mxi1* coding sequence covered.

In addition to SSCP analysis, we directly sequenced those exons that encode the helix-loop-helix and leucine zipper domains shown previously to be mutated in prostate tumors (5). Again, no mutations were detected. Although we were unable to detect *Mxi1* mutations in any of the tumors by either approach, we did detect a common

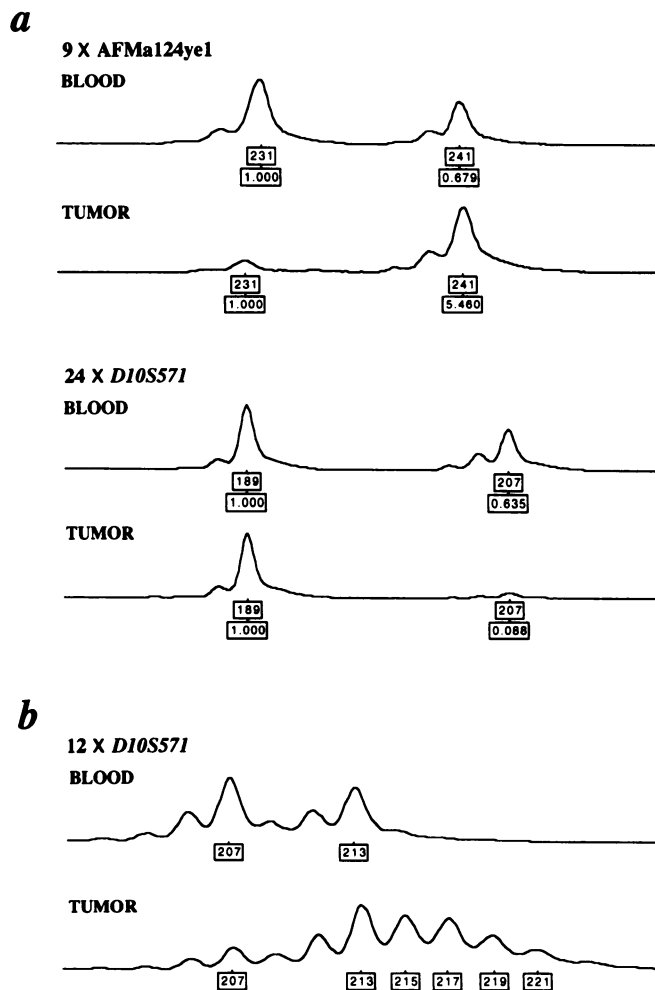


Fig. 1. *a*, examples of allelic loss at microsatellite markers on 10q23–25 in prostate tumors. The upper boxed figure beneath each peak gives the length of the allelic fragment; the lower box contains the relative peak height. “Shoulder” peaks to the left of the main peaks are due to polymerase slippage during PCR. *b*, microsatellite instability. Instability, thought to result from DNA mismatch repair errors (10), was seen in 1 of 37 tumors at 21 of 24 loci. Fragment lengths are given beneath each peak. The example shown here probably reflects deletion of the 207-bp allele in conjunction with expansion of the 213-bp allele.

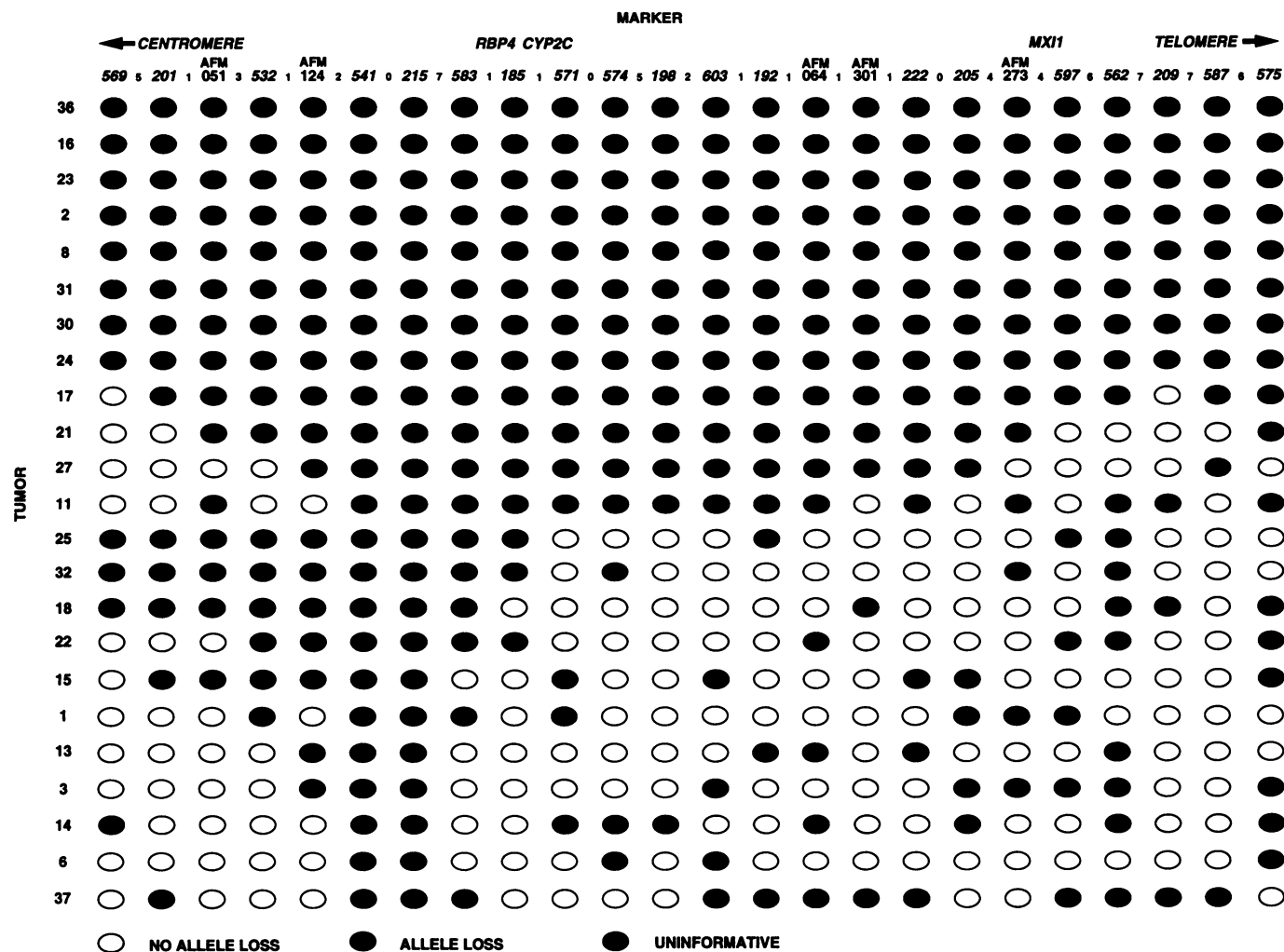


Fig. 2. Allelic loss at 10q23–25. Tumor numbers correspond to those in Table 1. Marker numbers in italics are *D10S* numbers (7). Markers denoted "AFM" have yet to be assigned *D* numbers; the full marker names are AFMa051tb9, AFMa124wd9, AFMa064za5, AFMa301ex1, and AFMa273ye1, respectively. Primer sequences for these markers will be described elsewhere.<sup>4</sup> Tumors 8, 16, 24, 30, and 31 also show allelic loss at markers *D10S189* and/or *D10S570* on the p arm of chromosome 10, implying whole chromosome loss. The smaller numbers give the approximate genetic distance between markers in cM. There is a clearly defined common region of deletion between markers AFMa124wd9 and *D10S583*, a distance of approximately 9 cM. In contrast, only tumors 1 and 11 show specific loss of markers around *Mxi1*; in both instances, this is in conjunction with allelic loss in the AFMa124wd9-*D10S583* region.

polymorphism<sup>1</sup> in the 3'-untranslated region by SSCP; subsequent sequence analysis showed that the polymorphism was a result of length variation in a (AAAAC)<sub>n</sub> tandem repeat, giving two alleles, (AAAAC)<sub>4</sub> and (AAAAC)<sub>5</sub>. Eight of the tumors showing loss of the entire 10q23–25 region or allelic loss at CA repeat markers in the vicinity of *Mxi1* (tumors 1, 8, 11, 16, 17, 21, 23, and 30) were heterozygous for this polymorphism, making it possible to assess these tumors for actual *Mxi1* loss. Six of the tumors (1, 8, 16, 17, 23, and 30) showing loss of adjacent markers also showed loss of *Mxi1*, as determined by fluorescence-based typing (Fig. 3). Of these tumors, 5 showed loss of the entire 10q24–25 region (Fig. 2). Therefore, from a total of 23 tumors showing 10q23–25 losses, we were able to identify only 1 tumor (tumor 1) showing specific deletion of *Mxi1* (as opposed to loss of other 10q23–25 regions or of the entire region), and this was in conjunction with deletion of AFMa124wd9-*D10S583*.

We were also able to use this polymorphism to determine the effect of contaminating normal tissue on the efficiency of mutation detection in tumors by cycle sequencing. Exon 5, including the immediate 3'-untranslated DNA, was sequenced in those tumors showing *Mxi1*

loss (tumors 1, 8, 16, 17, 23, and 30). For tumor 8, which showed the greatest degree of loss of the deleted allele, the retained allele was clearly identified. The remaining tumors gave highly ambiguous sequence data following the (AAAAC)<sub>n</sub> repeat, resulting from combined termination products from the two alleles (not shown). It is therefore likely that any disabling mutations resulting from small deletion or insertion events in the retained copies of *Mxi1* would have been detected by cycle sequencing.

## Discussion

The data presented here provide strong evidence for the presence of a prostate tumor suppressor gene(s) at the 10q23–24 boundary, and more specifically between markers AFMa124wd9 and *D10S583*, a region spanning approximately 9 cM. This region was deleted in 22 of 23 prostate tumors showing 10q losses; the 23rd tumor was uninformative for the relevant markers. 10q loss may be an early event in some instances of prostate carcinogenesis; losses were observed in early as well as late stage tumors. Alternatively, 10q loss may be more important in progression of the established tumor rather than genesis, given that losses were not observed in benign hyperplastic tissue

<sup>4</sup>J. Weissenbach, manuscript in preparation.

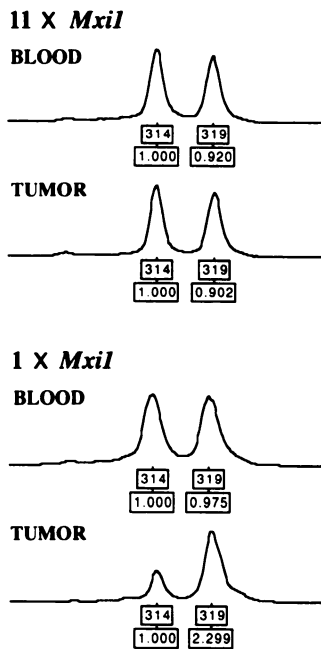


Fig. 3. *Mxi1* loss in prostate tumors. Assessment of allelic loss at the (AAAAC)<sub>n</sub> polymorphism in the 3'-untranslated region of the *Mxi1* gene in tumors 1 and 11, which show specific loss of adjacent microsatellite markers, by fluorescence-based typing. The boxed numbers beneath each peak give the allele fragment length (top) and relative peak height (bottom). Tumor 1 shows clear loss of *Mxi1* (peak height reduction, 58%), whereas tumor 11 shows no apparent loss of *Mxi1*, despite showing loss of adjacent microsatellite marker AFMa273ye1.

samples. However, the relationship between benign prostatic hyperplasia and carcinogenesis is unclear at present, and such lesions may not be a precursor to malignancy.

Although *Mxi1* has been shown to be mutated in prostate tumors, only a small proportion of cells in each tumor were found to be carrying *Mxi1* mutations (5). The authors offer two possible explanations: (a) the tumors studied may have contained significant amounts of nonneoplastic tissue; or (b) mutated *Mxi1* alleles are only present in a small number of neoplastic cells. Given that we were unable to detect *Mxi1* mutations in microdissected tumors containing <30% contaminating normal tissue and showing a degree of 10q loss ranging from 25–79% (as estimated by microsatellite allelic loss; see Table 1), the latter seems more likely. This also implies that mutation of the retained *Mxi1* allele occurs after loss of the deleted allele. Although the mutation analyses presented here are clearly not exhaustive, we feel that the combined evidence of no mutation detection, or detection in only a small percentage of tumor cells, coupled with the allelic loss data, points to the presence of a tumor suppressor gene(s) at 10q23–24 of greater significance than *Mxi1* in prostate tumor progression.

Loss or rearrangement of 10q24–25 is not restricted to prostate adenocarcinoma; it has also been observed in melanoma, glioma and non-Hodgkin's lymphoma (15–21), suggesting the presence of a tumor suppressor gene(s) at this location of relevance to several tumor types. Further allelic loss studies of a range of different tumor types,

together with *Mxi1* mutation analysis, should help to clarify the role of 10q23–25 in tumor pathogenesis and progression.

### Acknowledgments

We thank David Kelsell for helpful discussions and Iain Goldsmith and colleagues for oligonucleotide synthesis.

### References

- Cannon-Albright, L., and Eeles, R. Progress in prostate cancer. *Nat. Genet.*, 9: 336–338, 1995.
- Lundgren, R., Mandahl, N., Heim, S., Limon, J., Henrikson, H., and Mitelman, F. Cytogenetic analysis of 57 primary prostatic adenocarcinomas. *Genes Chromosomes & Cancer*, 4: 16–24, 1992.
- Arps, S., Rodewald, A., Schmalenberger, B., Carl, P., Bressel, M., and Kastendieck, H. Cytogenetic survey of 32 cancers of the prostate. *Cancer Genet. Cytogenet.*, 66: 93–99, 1993.
- Zervos, S. J., Gyuris, J., and Brent, R. *Mxi1*, a protein that specifically interacts with Max to bind Myc-Max recognition sites. *Cell*, 72: 223–232, 1993.
- Eagle, L. R., Yin, X., Brothman, A. R., Williams, B. J., Atkin, N. B., and Prochownik, E. V. Mutation of the *Mxi1* gene in prostate cancer. *Nat. Genet.*, 9: 249–255, 1995.
- Phillips, S. M. A., Morton, D. G., Lee, S. J., Wallace, D. M. A., and Neoptolemos, J. P. Loss of heterozygosity of the retinoblastoma and adenomatous polyposis susceptibility gene loci and in chromosomes 10p, 10q, and 16q in human prostate cancer. *Br. J. Urol.*, 73: 390–395, 1994.
- Gyapay, G., Morissette, J., Vignal, A., Dib, C., Fizames, C., Millasseau, P., Marc, S., Bernardi, G., Lathrop, M., and Weissenbach, J. The 1993–1994 Genethon human genetic linkage map. *Nat. Genet.*, 7: 246–339, 1994.
- Orita, M., Iwahana, H., Kanazawa, H., Hayashi, K., and Sekiya, T. Detection of polymorphisms of human DNA by gel electrophoresis as single-strand conformation polymorphisms. *Proc. Natl. Acad. Sci. USA*, 86: 2766–2770, 1989.
- Union Internationale Contre Le Cancer. *TNM Classification of Malignant Tumours*. Geneva: International Union Against Cancer, 1978.
- Parsons, R., Li, G.-M., Longley, M. J., Fang, W., Papadopoulos, N., Jen, J., de la Chapelle, A., Kinzler, K. W., Vogelstein, B., and Modrich, P. Hypermutability and mismatch repair deficiency in RER+ tumor cells. *Cell*, 75: 1227–1236, 1993.
- Gray, I. C., Nobile, C., Moresu, R., Ford, S., and Spurr, N. K. A 2.4 megabase physical map spanning the *CYP2C* gene cluster on chromosome 10q24. *Genomics* 28: 328–332, 1995.
- Rocchi, M., Covone, A., Romeo, G., Faraonio, R., and Colantuoni, V. Regional mapping of *RBP4* to 10q23–24 and *RBP1* to 3q21–22 in man. *Somatic Cell Mol. Genet.*, 15: 185–190, 1989.
- Inoue, K., Inazawa, J., Suzuki, Y., Shimada, T., Yamazaki, H., Guengerich, F. P., and Abe, T. Fluorescence *in-situ* hybridization analysis and chromosomal localization of 3 human cytochrome-p450-2c genes (*cyp2c8*, *2c9* and *2c10*) at 10q24.1. *Jpn. J. Hum. Genet.*, 39: 337–343, 1994.
- Cohen, D., Chumakov, I., and Weissenbach, J. A first generation physical map of the human genome. *Nature (Lond.)*, 366: 698–701, 1993.
- Parmiter, A. H., Balaban, G., Clark, W. H. J., and Nowell, P. C. Possible involvement of the chromosome region 10q24–q26 in early stages of melanocytic neoplasia. *Cancer Genet. Cytogenet.*, 30: 313–317, 1988.
- Ransom, D. T., Ritland, S. R., Moertel, C. A., Dahl, R. J., O'Fallon, J. R., Scheithauer, B. W., Kimmel, D. W., Kelly, P. J., Olopade, O. I., Diaz, M. O., and Jenkins, R. B. Correlation of cytogenetic analysis and loss of heterozygosity studies in human diffuse astrocytomas and mixed oligo-astrocytomas. *Genes Chromosomes & Cancer*, 5: 357–374, 1992.
- Rasheed, B. K. A., Fuller, G. N., Friedman, A. H., Bigner, D. D., and Bigner, S. H. Loss of heterozygosity for 10q loci in human gliomas. *Genes Chromosomes & Cancer*, 5: 75–82, 1992.
- Speaks, S. L., Sanger, W. G., Masih, A. S., Harrington, D. S., Hess, M., and Armitage, J. O. Recurrent abnormalities of chromosome bands 10q23–q25 in non-Hodgkin's lymphoma. *Genes Chromosomes & Cancer*, 5: 239–243, 1992.
- Fults, D., and Pedone, C. Deletion mapping of the long arm of chromosome 10 in glioblastoma multiforme. *Genes Chromosomes & Cancer*, 7: 173–177, 1993.
- Karlbom, A. E., James, C. D., Boethius, J., Cavenee, W. K., Collins, V. P., Nordenskjold, M., and Larsson, C. Loss of heterozygosity in malignant gliomas involves at least three distinct regions on chromosome 10. *Hum. Genet.*, 92: 169–174, 1993.
- Herbst, R. A., Weiss, J., Ehnis, A., Cavane, W. K., and Arden, K. C. Loss of heterozygosity for 10q22–10qter in malignant melanoma progression. *Cancer Res.*, 54: 3111–3114, 1994.

# Cancer Research

The Journal of Cancer Research (1916–1930) | The American Journal of Cancer (1931–1940)

## Loss of the Chromosomal Region 10q23–25 in Prostate Cancer

Ian C. Gray, Stewart M. A. Phillips, Susan J. Lee, et al.

*Cancer Res* 1995;55:4800-4803.

**Updated version** Access the most recent version of this article at:  
<http://cancerres.aacrjournals.org/content/55/21/4800>

**E-mail alerts** [Sign up to receive free email-alerts](#) related to this article or journal.

**Reprints and Subscriptions** To order reprints of this article or to subscribe to the journal, contact the AACR Publications Department at [pubs@aacr.org](mailto:pubs@aacr.org).

**Permissions** To request permission to re-use all or part of this article, use this link <http://cancerres.aacrjournals.org/content/55/21/4800>. Click on "Request Permissions" which will take you to the Copyright Clearance Center's (CCC) Rightslink site.